

Bozonized Momentum Distribution of a Fermi Gas via Friedrichs Diagrams

Sascha Lill^{1,*}

¹*ORCID: 0000-0002-9474-9914, e-mail: sascha.lill@unimi.it*

** Università degli Studi di Milano, Dipartimento di Matematica, Via Cesare Saldini 50, 20133 Milano, Italy*

November 21, 2023

Abstract

Recently [1], Benedikter and the author proved an approximate formula for the momentum distribution of a 3d fermionic gas interacting by a short-range pair potential in the mean-field regime, within a trial state close to the ground state. Here, we derive an exact formula for the momentum distribution in this trial state, using a diagrammatic formalism due to Friedrichs. We further demonstrate how the formula of Benedikter and the author arises from a restriction of the contributing diagrams to those corresponding to a bosonization approximation.

Keywords: Fermi gas; many-body quantum mechanics; momentum distribution; bosonization; Friedrichs diagrams; diagrammatic expansions.

Contents

1	Introduction	2
2	Bosonized Operators and Trial State	4
3	Momentum Distribution	8
4	Friedrichs Diagram Formalism	13
5	Multicommutator Evaluation via Friedrichs Diagrams	16
6	Bosonization Approximation in Friedrichs Diagrams	22

2020 *Mathematics Subject Classification.* 81V70, 81V74, 81Q12, 81S05.

1 Introduction

In recent years, there has been a surge of interest in the mathematical research on three-dimensional (3d) fermionic quantum gases, employing bosonization techniques. Generally, such a system comprises N fermions on a 3d torus, $\mathbb{T}^3 := [0, L]^3$, whose state is described by a vector

$$\psi \in L^2_{\mathfrak{a}}(\mathbb{T}^{3N}) := \left\{ \psi \in L^2(\mathbb{T}^{3N}) \mid \psi(\dots, x_i, \dots, x_j, \dots) = -\psi(\dots, x_j, \dots, x_i, \dots) \forall 1 \leq i < j \leq n \right\}. \quad (1)$$

The system is modeled by a Hamiltonian operator of the form

$$H_N := \sum_{j=1}^N -\hbar^2 \Delta_{x_j} + \lambda \sum_{i < j}^N V(x_i - x_j), \quad (2)$$

with a sufficiently regular pair potential $V : \mathbb{R}^3 \rightarrow \mathbb{R}$, and where $\hbar > 0$ is the semiclassical constant and $\lambda > 0$ the coupling constant. For a given density $\rho := \frac{N}{L^3}$, we require the energy to be extensive, which fixes $\hbar \sim \rho^{-\frac{1}{3}}$ and $\lambda \sim \rho^{-1}$.

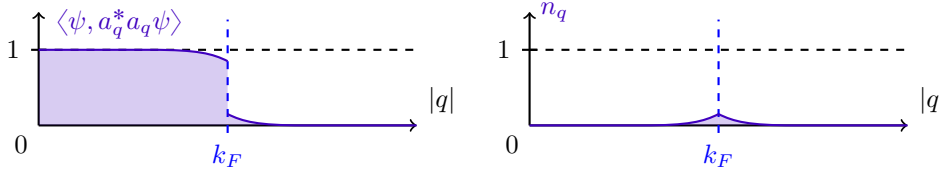


Figure 1: Left: Schematic depiction of the momentum distribution $\langle \psi, a_q^* a_q \psi \rangle$, where the Fermi momentum k_F is the radius of the Fermi ball $B_F = \overline{B_{k_F}(0)}$.

Right: Excitation density n_q for the same trial state ψ .

Since physical systems often feature large particle numbers, it is of particular interest to derive mathematical statements in the limit $N = \rho L^3 \rightarrow \infty$. Evidently, there are several choices of sequences in (ρ, L) for which $N \rightarrow \infty$, where we will focus on the **mean-field limit** characterized by

$$L := 2\pi, \quad \hbar := N^{-\frac{1}{3}}, \quad \lambda := N^{-1}, \quad \rho \rightarrow \infty. \quad (3)$$

We consider a sequence of trial states $\psi_N = \psi$, first introduced in [2] and close to the ground state. The quantity we are interested in is the **momentum distribution** $q \mapsto \langle \psi, a_q^* a_q \psi \rangle \in [0, 1]$, with momentum $q \in \mathbb{Z}^3$ and where a_q^*, a_q are the fermionic creation and annihilation operators defined below. Physically, $\langle \psi, a_q^* a_q \psi \rangle$ describes the probability that a momentum mode q is occupied. It is well-known that for $\lambda = 0$, this probability is 1 if q is inside the Fermi ball $B_F := \overline{B_{k_F}(0)}$ for some Fermi momentum

k_F , and 0 outside B_F . The deviation from this profile for $\lambda > 0$ is called **excitation density**

$$n_q := \begin{cases} \langle \psi, a_q^* a_q \psi \rangle & \text{for } q \in B_F^c \\ 1 - \langle \psi, a_q^* a_q \psi \rangle & \text{for } q \in B_F \end{cases}, \quad (4)$$

see Fig. 1. n_q is expected to be small for small λ , and it fully characterizes the momentum distribution. Our **main result**, Theorem 1, is now an exact formula for n_q in terms of so-called Friedrichs diagrams. Morally, it reads

$$n_q = \sum_{\text{diagrams}} \text{value of the diagram}, \quad (5)$$

with the sum being infinite but convergent. Friedrichs diagrams are a convenient tool to facilitate computationally intensive (anti-)commutator evaluations. They first appeared in [18] and soon found a widespread application in constructive quantum field theory (CQFT) [24, 22, 23, 17]. For further information on Friedrichs diagrams, we refer the interested reader to [8, 15].

Theorem 1 complements a recent result in [1], where an approximate excitation density $n_q^{(b)}$ was derived using a bosonization technique, and proven to be the correct leading order expression for n_q . We will demonstrate in Proposition 1 how $n_q^{(b)}$ arises from an intuitive restriction to certain “bosonized diagrams” as

$$n_q^{(b)} = \sum_{\text{bosonized diagrams}} \text{value of the diagram}. \quad (6)$$

Let us remark that a similar diagrammatic formalism was applied in the early physics literature for deriving the ground state energy of a Fermi gas with Coulomb interaction (Jellium) at high densities [19, 29, 14]. In particular, [14] employs a Feynman–Hellmann argument to obtain formulas for the momentum distribution, which agree with the one implied by $n_q^{(b)}$ for short-ranged interactions, see [1, Appendix B]. However, the formalism in [19, 29, 14] corresponds to Feynman diagrams rather than Friedrichs diagrams: Lines represent propagators rather than Kronecker deltas and vertices represent interactions in the interaction picture at distinct times.

Other results in the physics literature on the ground state energy of a 3d Fermi gas include [6, 7, 30, 12, 13, 25]. From [25], further formulas for the momentum distribution involving spin were derived by a Feynman–Hellmann argument in [26].

The trial state we use is of the form $\psi = RT\Omega$ with R being a particle-hole transformation and T an “almost bosonic” Bogoliubov transformation, based on a patch construction, which we describe below in Sect. 2. It was first used in [2] to derive an upper bound on the ground state energy of a 3d mean-field Fermi gas, with¹ $\text{supp}\hat{V}$ being compact. The same construction was shortly afterwards used to provide a matching

¹Here, \hat{V} denotes the Fourier transform of V .

lower bound for weak interactions (compact $\text{supp}\hat{V}$ and $\|\hat{V}\|_\infty$ small) [3] and stronger interactions ($\sum_k |k|\hat{V}(k) < \infty$) [5], as well as for a description of the dynamics generated by H_N with $\text{supp}\hat{V}$ compact [4]. Another almost bosonic Bogoliubov transformation similar to T , but not depending on a patch construction, was introduced in [9], allowing for an upper and lower bound on the ground state energy in case $\sum_k |k|\hat{V}(k) < \infty$. This transformation was employed to determine the lower excitation spectrum [10] and proving an upper bound on the ground state energy [11], both in case $\sum_k \hat{V}(k)^2 < \infty$. This case also covers the Coulomb case $\hat{V}(k) = |k|^{-2}$ for $k \neq 0$ and $\hat{V}(0) = 0$, also called Jellium model. Note that all references above in this paragraph assume $\hat{V} \geq 0$.

Another way to send $N \rightarrow \infty$ for a 3d Fermi gas (2) is given by the thermodynamic limit, where one fixes ρ and takes $L \rightarrow \infty$. Here, in the dilute regime ($\rho \ll 1$), further “almost bosonic” Bogoliubov transformations have been introduced, which are based on solutions of the scattering equation. They allow for proving upper and lower bounds on the ground state energy for smooth $V \geq 0$ [16, 20, 21].

The proof of ground state energy formulas in the thermodynamic limit for large ρ remains a challenging open problem. Also, the rigorous establishment of momentum distribution formulas for the true ground state, rather than just some trial state ψ , is an interesting open task.

Let us further remark that in the 1d Luttinger model [28], the exact momentum distribution for the ground state has been obtained long ago [27], as the model is exactly solvable.

The rest of this article is structured as follows. In Sect. 2 we introduce the mathematical notation that is needed to define the trial state ψ in (11). Sect. 3 contains our main result, Theorem 1, as well as Proposition 2, preceded by the minimal definitions needed to write down the diagrammatic contributions. The actual Friedrichs diagram formalism is introduced in Sect. 4. It allows us to prove Theorem 1 in Sect. 5, where it also becomes clear how the diagrammatic contributions arise from actual diagrams. In Sect. 6, we heuristically motivate why the largest contributions to n_q come from the “bosonized” diagrams in $n_q^{(b)}$, and we finally prove Proposition 1.

2 Bosonized Operators and Trial State

We mostly adopt the setting of [1]. It is well-known that in the non-interacting case, $V = 0$, one ground state of H_N is given by a Slater determinant, called Fermi ball state

$$\psi_{\text{FB}}(x_1, x_2, \dots, x_N) := \frac{1}{\sqrt{N!}} \det \left(\frac{1}{(2\pi)^{3/2}} e^{ik_j \cdot x_i} \right)_{j,i=1}^N, \quad (7)$$

with disjoint momenta $(k_j)_{j=1}^N \subset \mathbb{Z}^3$ minimizing the kinetic energy $\sum_{j=1}^N \hbar^2 |k_j|^2$. More precisely, the k_j occupy the Fermi ball

$$B_F := \{k \in \mathbb{Z}^3 \mid |k| \leq k_F\} \quad \text{for some Fermi momentum } k_F > 0, \quad (8)$$

where in particular, we assume² $N = |B_F|$.

For $V \neq 0$, the true ground state of H_N has a highly non-trivial structure. We will therefore approximate it by the (N -dependent) trial state $\psi = \psi_N$ introduced in [2]. To define ψ , it is convenient to work in the language of second quantization. To this end, we introduce the fermionic Fock space

$$\mathcal{F} := \bigoplus_{n=0}^{\infty} L_a^2(\mathbb{T}^{3n}),$$

and the orthonormal plane wave basis $(f_q)_{q \in \mathbb{Z}^3} \subset L^2(\mathbb{T}^3)$ with $f_q(x) := (2\pi)^{-\frac{3}{2}} e^{iq \cdot x}$, $q \in \mathbb{Z}^3$ and the corresponding creation and annihilation operators

$$a_q^*, a_q : \mathcal{F} \rightarrow \mathcal{F}, \quad a_q^* := a^*(f_q), \quad a_q := a(f_q),$$

which satisfy the canonical anticommutation relations (CAR)

$$\{a_q, a_{q'}^*\} = \delta_{q,q'}, \quad \{a_q, a_{q'}\} = \{a_q^*, a_{q'}^*\} = 0 \quad \text{for all } q, q' \in \mathbb{Z}^3. \quad (9)$$

The vacuum vector $\Omega \in \mathcal{F}$ is given by $\Omega := (1, 0, 0, \dots)$ and satisfies $a_q \Omega = 0$ for all $q \in \mathbb{Z}^3$. Further, the Fermi ball state ψ_{FB} (7) can now conveniently be written as $\psi_{\text{FB}} = R\Omega$ with $R = R^* : \mathcal{F} \rightarrow \mathcal{F}$ being a unitary **particle-hole transformation** defined via

$$R^* a_q^* R := \begin{cases} a_q^* & \text{if } q \in B_F^c \\ a_q & \text{if } q \in B_F \end{cases}. \quad (10)$$

By contrast, our **trial state** is of the form

$$\psi := RT\Omega, \quad \psi \in L_a^2(\mathbb{T}^{3N}) \subset \mathcal{F}, \quad (11)$$

where $T : \mathcal{F} \rightarrow \mathcal{F}$ is a unitary ‘‘almost bosonic Bogoliubov transformation’’, which we define in the following.

The first step in the definition of T consists of constructing M **patches** $B_1, \dots, B_M \subset \mathbb{R}^3$ around the Fermi surface ∂B_F , see Fig. 2. Details of the construction are given in [2, 3] and involve some fixed constant $R > 0$. Each patch covers approximately the same surface area of $\frac{4\pi k_F^2}{M}$, has a thickness of $2R$, and is separated from the neighboring

²That is, when taking $N \rightarrow \infty$, we restrict to a sequence $(N_n)_{n \in \mathbb{N}}$ such that $N_n = |\overline{B_{k_F^{(n)}}(0)} \cap \mathbb{Z}^3|$ for some $(k_F^{(n)})_{n \in \mathbb{N}} \subset \mathbb{R}$

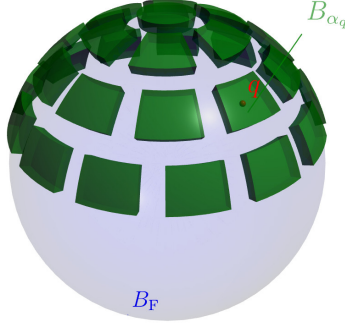


Figure 2: Patches on the Fermi ball in momentum space.

patches by a corridor of width $> R$. Its edges are assumed to be regular in the sense that

$$\text{diam}(B_\alpha) \leq CN^{\frac{1}{3}}M^{-\frac{1}{2}},$$

and the patch number M is chosen such that $N^{2\delta} \ll M \ll N^{\frac{2}{3}-2\delta}$ for some $0 < \delta < \frac{1}{6}$. Denoting the center of a patch B_α by $\omega_\alpha \in \mathbb{R}^3$ with corresponding unit vector $\hat{\omega}_\alpha := \frac{\omega_\alpha}{|\omega_\alpha|}$, we define for every fixed $k \in \mathbb{Z}^3$ the index sets

$$\begin{aligned} \mathcal{I}_k^+ &:= \{\alpha \in \{1, \dots, M\} \mid k \cdot \hat{\omega}_\alpha \geq N^{-\delta}\}, \\ \mathcal{I}_k^- &:= \{\alpha \in \{1, \dots, M\} \mid k \cdot \hat{\omega}_\alpha \leq -N^{-\delta}\}, \\ \mathcal{I}_k &:= \mathcal{I}_k^+ \cup \mathcal{I}_k^-. \end{aligned} \quad (12)$$

The patch construction is assumed to be symmetric under replacement $k \mapsto -k$, so we have $|\mathcal{I}_k^+| = |\mathcal{I}_k^-| \leq \frac{M}{2}$. The symmetry allows us to restrict our focus to momenta k within the northern half-sphere

$$H^{\text{nor}} := \{k \in \mathbb{R}^3 \mid k_3 > 0 \text{ or } (k_3 = 0 \text{ and } k_2 > 0) \text{ or } (k_3 = k_2 = 0 \text{ and } k_1 > 0)\}. \quad (13)$$

Let us further adopt the following conventions: All momenta k, q, p, h are assumed to be elements of \mathbb{Z}^3 . For $p \in \mathbb{Z}^3$ (“particle”), the condition $p \in B_F^c \cap B_\alpha$ is abbreviated as $p : \alpha$ (read as “ p is compatible with B_α ”) and for $h \in \mathbb{Z}^3$ (“hole”), the condition $h \in B_F \cap B_\alpha$ is abbreviated as $h : \alpha$. Further, we introduce the notation

$$\pm k := \begin{cases} +k & \text{if } \alpha \in \mathcal{I}_k^+ \\ -k & \text{if } \alpha \in \mathcal{I}_k^- \end{cases} \quad \text{and} \quad \mp k := \begin{cases} -k & \text{if } \alpha \in \mathcal{I}_k^+ \\ +k & \text{if } \alpha \in \mathcal{I}_k^- \end{cases}.$$

Given a momentum transfer

$$k \in \Gamma^{\text{nor}} := H^{\text{nor}} \cap \mathbb{Z}^3 \cap B_R(0), \quad (14)$$

the number of particle–hole pairs with $p = h \pm k$ in patch $B_\alpha \in \mathcal{I}_k$ is then

$$n_{\alpha,k}^2 := \sum_{p,h:\alpha} \delta_{p,h\pm k} = \sum_{\substack{p:p \in B_F^c \cap B_\alpha \\ p \mp k \in B_F \cap B_\alpha}} 1. \quad (15)$$

We now define for $k \in \Gamma^{\text{nor}}$ and $B_\alpha \in \mathcal{I}_k$ the **almost bosonic creation operator**

$$c_\alpha^*(k) := \frac{1}{n_{\alpha,k}} \sum_{p,h:\alpha} \delta_{p,h\pm k} a_p^* a_h^* = \frac{1}{n_{\alpha,k}} \sum_{\substack{p:p \in B_F^c \cap B_\alpha \\ p \mp k \in B_F \cap B_\alpha}} a_p^* a_{p \mp k}^* , \quad (16)$$

with its adjoint being $c_\alpha(k)$. The normalization factor $n_{\alpha,k}$ is precisely chosen such that c^*, c satisfy the **approximate canonical commutation relations** (CCR) [1, 2, 3]

$$[c_\alpha(k), c_\beta^*(\ell)] = \begin{cases} 0 & \text{if } \alpha \neq \beta \\ \delta_{k,\ell} + \mathcal{E}_\alpha(k, \ell) & \text{if } \alpha = \beta \end{cases} , \quad (17)$$

with commutation error

$$\mathcal{E}_\alpha(k, \ell) := - \sum_{p,h_1,h_2:\alpha} \frac{\delta_{h_1,p \mp k} \delta_{h_2,p \mp \ell}}{n_{\alpha,k} n_{\alpha,\ell}} a_{h_2}^* a_{h_1} - \sum_{p_1,p_2,h:\alpha} \frac{\delta_{h,p_1 \mp k} \delta_{h,p_2 \mp \ell}}{n_{\alpha,k} n_{\alpha,\ell}} a_{p_2}^* a_{p_1} . \quad (18)$$

The **almost bosonic Bogoliubov transformation** $T : \mathcal{F} \rightarrow \mathcal{F}$ generating the trial state $\psi = RT\Omega$ is then of the form

$$T := e^{-S} , \quad S := -\frac{1}{2} \sum_{k \in \Gamma^{\text{nor}}} \sum_{\alpha, \beta \in \mathcal{I}_k} K(k)_{\alpha, \beta} (c_\alpha^*(k) c_\beta^*(k) - \text{h.c.}) , \quad (19)$$

with $K(k) \in \mathbb{R}^{|\mathcal{I}_k| \times |\mathcal{I}_k|}$ being a symmetric matrix defined below. So $S^* = -S$ and

$$\begin{aligned} S &= S_+ + S_- , \quad \text{where } S_- = -(S_+)^* \text{ and} \\ S_+ &:= -\frac{1}{2} \sum_{k \in \Gamma^{\text{nor}}} \sum_{\alpha, \alpha' \in \mathcal{I}_k} K(k)_{\alpha, \alpha'} \sum_{\substack{p,h:\alpha \\ p',h':\alpha'}} \frac{\delta_{p,h\pm k} \delta_{p',h'\pm k}}{n_{\alpha,k} n_{\alpha',k}} a_p^* a_h^* a_{p'}^* a_{h'}^* . \end{aligned} \quad (20)$$

The motivation behind the definition of T is to “almost-diagonalize” some effective quadratic bosonic Hamiltonian, see [2, 3]. This requires the following choice of k -dependent matrices:

$$\begin{aligned} K &:= \log |S_1^T| , \\ S_1 &:= (D + W - \widetilde{W})^{\frac{1}{2}} E^{-\frac{1}{2}} , \\ E &:= \left((D + W - \widetilde{W})^{\frac{1}{2}} (D + W + \widetilde{W}) (D + W - \widetilde{W})^{\frac{1}{2}} \right)^{\frac{1}{2}} , \end{aligned} \quad (21)$$

with the $\mathbb{R}^{|\mathcal{I}_k| \times |\mathcal{I}_k|}$ symmetric block matrices

$$D = \begin{pmatrix} d & 0 \\ 0 & d \end{pmatrix} , \quad W = \begin{pmatrix} b & 0 \\ 0 & b \end{pmatrix} , \quad \widetilde{W} = \begin{pmatrix} 0 & b \\ b & 0 \end{pmatrix} ,$$

where $d, b \in \mathbb{R}^{|\mathcal{I}_k^+| \times |\mathcal{I}_k^+|}$ are given by

$$d := \sum_{\alpha \in \mathcal{I}_k^+} |\hat{k} \cdot \hat{\omega}_\alpha| |\alpha\rangle\langle\alpha|, \quad b := \sum_{\alpha, \beta \in \mathcal{I}_k^+} \frac{\hat{V}(k)}{2\hbar\kappa N|k|} n_{\alpha,k} n_{\beta,k} |\alpha\rangle\langle\beta|. \quad (22)$$

Here, $|\alpha\rangle \in \mathbb{R}^{|\mathcal{I}_k^+|}$ is the α -th canonical basis vector, we have $\hat{k} := k/|k|$ and $\kappa := k_{\text{F}} N^{-\frac{1}{3}} \approx \left(\frac{3}{4\pi}\right)^{\frac{1}{3}}$. This concludes the construction of the trial state ψ .

3 Momentum Distribution

In [1, Thm. 3.1], it was proved that for $\hat{V} \geq 0$ compactly supported, the excitation density n_q (4) is approximately given by some **bosonized excitation density** [1, (5.7)] of the form

$$n_q^{(\text{b})} := \frac{1}{2} \sum_{k \in \tilde{\mathcal{C}}^q \cap \mathbb{Z}^3} \frac{1}{n_{\alpha_q, k}^2} (\cosh(2K(k)) - 1)_{\alpha_q, \alpha_q}, \quad (23)$$

in the sense that for fixed V ,

$$|n_q - n_q^{(\text{b})}| \leq C_\varepsilon N^{-\frac{5}{6} + \frac{5}{4}\delta + \varepsilon}, \quad (24)$$

with $C_\varepsilon > 0$ depending only on $\varepsilon > 0$ and not on N . Here $\tilde{\mathcal{C}}^q$ [1, (3.1)] is defined such that

$$\tilde{\mathcal{C}}^q \cap \mathbb{Z}^3 = \begin{cases} \{k \in \Gamma^{\text{nor}} \mid \alpha_q \in \mathcal{I}_k \text{ and } q \mp k : \alpha_q\} & \text{if } q \in B_{\text{F}}^c \\ \{k \in \Gamma^{\text{nor}} \mid \alpha_q \in \mathcal{I}_k \text{ and } q \pm k : \alpha_q\} & \text{if } q \in B_{\text{F}} \end{cases}. \quad (25)$$

The approximation $n_q^{(\text{b})}$ arises when evaluating the multicommutator series

$$n_q = \langle \Omega, T^* a_q^* a_q T \Omega \rangle = \langle \Omega, e^S a_q^* a_q e^{-S} \Omega \rangle = \sum_{n=0}^{\infty} \frac{1}{n!} \langle \Omega, \text{ad}_S^n(a_q^* a_q) \Omega \rangle, \quad (26)$$

with $\text{ad}_A^n(B) = [A, \dots, [A, [A, B]] \dots]$ being the n -fold multicommutator.

We will now provide an exact formula (38) for n_q , which requires introducing some notation. It turns out that only even n render contributions to n_q in (26). For such n , we denote the momenta of the n involved S -operators, see (20), by $\{p_j, p'_j, h_j, h'_j\}_{j=1}^n$. For later convenience we write

$$a_q^* a_q = \begin{cases} \sum_{p_0, p'_0} \delta_{q, p_0} \delta_{q, p'_0} a_{p_0}^* a_{p'_0} & \text{for } q \in B_{\text{F}}^c \\ \sum_{h_0, h'_0} \delta_{q, h_0} \delta_{q, h'_0} a_{h_0}^* a_{h'_0} & \text{for } q \in B_{\text{F}} \end{cases}, \quad (27)$$

which allows to write the involved momentum indices in the multicommutator as

$$\begin{aligned} \mathbf{P} &:= (p_0, p_1, \dots, p_n), & \mathbf{P}' &:= (p'_0, p'_1, \dots, p'_n), \\ \mathbf{H} &:= (h_1, \dots, h_n), & \mathbf{H}' &:= (h'_1, \dots, h'_n), \end{aligned} \quad (28)$$

for $q \in B_{\mathbb{F}}^c$. In case $q \in B_{\mathbb{F}}$, we analogously include h_0 and h'_0 into \mathbf{H} and \mathbf{H}' . We will further split each commutator with $S = S_+ + S_-$ (20) into one commutator with S_+ and one with S_- , where the choices between S_+ or S_- are tracked by a map

$$\xi \in \Xi_n := \left\{ \xi : \{1, \dots, n\} \mapsto \{1, -1\} \mid \sum_{j=1}^n \xi(j) = 0 \right\}. \quad (29)$$

Here, $\xi(j) = 1$ means that S_+ and $\xi(j) = -1$ that S_- is chosen for the j -th commutator. According to $\xi \in \Xi_n$, we may split the momentum indices into those belonging to creation and annihilation parts. In case $q \notin B_{\mathbb{F}}$,

$$\begin{aligned} \mathbf{P} &= \mathbf{P}_+ \cup \mathbf{P}_-, & \mathbf{P}_+ &:= p_0 \cup (p_j : \xi(j) = 1), & \mathbf{P}_- &:= (p_j : \xi(j) = 0), \\ \mathbf{H} &= \mathbf{H}_+ \cup \mathbf{H}_-, & \mathbf{H}_+ &:= (h_j : \xi(j) = 1), & \mathbf{H}_- &:= (h_j : \xi(j) = 0), \\ \mathbf{P}' &= \mathbf{P}'_+ \cup \mathbf{P}'_-, & \mathbf{P}'_+ &:= (p'_j : \xi(j) = 1), & \mathbf{P}'_- &:= p'_0 \cup (p'_j : \xi(j) = 0), \\ \mathbf{H}' &= \mathbf{H}'_+ \cup \mathbf{H}'_-, & \mathbf{H}'_+ &:= (h'_j : \xi(j) = 1), & \mathbf{H}'_- &:= (h'_j : \xi(j) = 0). \end{aligned} \quad (30)$$

In case $q \in B_{\mathbb{F}}$, we analogously include h_0 in \mathbf{H}_+ and h'_0 in \mathbf{H}'_- .

The contractions will now each be between one creation- (+) and one annihilation momentum index (-). We track them by two bijective maps

$$\pi_p : \mathbf{P}_- \cup \mathbf{P}'_- \mapsto \mathbf{P}_+ \cup \mathbf{P}'_+, \quad \pi_h : \mathbf{H}_- \cup \mathbf{H}'_- \mapsto \mathbf{H}_+ \cup \mathbf{H}'_+. \quad (31)$$

All contractions are subject to the constraint that for each S_{\pm} -operator, at least one momentum index is contracted to an ‘‘earlier’’ index:

$$\begin{aligned} \forall j \in \{1, \dots, n\} \exists \ell \in \{0, \dots, j-1\} : \\ \left\{ \begin{array}{ll} \{\pi_p(p_\ell), \pi_p(p'_\ell), \pi_h(h_\ell), \pi_h(h'_\ell)\} \cap \{p_j, p'_j, h_j, h'_j\} \neq \emptyset & \text{if } \xi(j) = 1 \\ \{\pi_p(p_j), \pi_p(p'_j), \pi_h(h_j), \pi_h(h'_j)\} \cap \{p_\ell, p'_\ell, h_\ell, h'_\ell\} \neq \emptyset & \text{if } \xi(j) = -1 \end{array} \right\}. \end{aligned} \quad (32)$$

The emergence of this constraint will become apparent later in Sect. 5. We then denote the set of **admissible contraction choices** by

$$\Pi_n^{(\xi)} := \{(\pi_p, \pi_h) \mid (32) \text{ holds}\}. \quad (33)$$

To each contraction choice, we will now associate a sign factor $\text{sgn}(\xi, \pi_p, \pi_h) \in \{1, -1\}$. In order to define this sign factor, let us introduce the sets of creation- and annihilation associated momenta

$$\mathbf{Q}_+ := \mathbf{P}_+ \cup \mathbf{P}'_+ \cup \mathbf{H}_+ \cup \mathbf{H}'_+, \quad \mathbf{Q}_- := \mathbf{P}_- \cup \mathbf{P}'_- \cup \mathbf{H}_- \cup \mathbf{H}'_-, \quad (34)$$

as well as two ordering relations $<$ on \mathbf{Q}_- and on \mathbf{Q}_+ , respectively, defined by

$$\ell < j \Rightarrow p_\ell, h_\ell, p'_\ell, h'_\ell < p_j, h_j, p'_j, h'_j \quad \text{and} \quad p_j < h_j < p'_j < h'_j. \quad (35)$$

To each contraction choice, we associate a sign factor

$$\text{sgn}(\xi, \pi_p, \pi_h) := \prod_{q_- \in \mathcal{Q}_-} \prod_{\substack{q'_- \in \mathcal{Q}_- \\ q'_- > q_-, \pi_{\sharp}(q'_-) < \pi_{\sharp}(q_-)}} (-1), \quad (36)$$

with $\sharp \in \{p, h\}$, according to whether q_-, q'_- are particle or hole momenta. Finally, let us abbreviate the momentum transfer and patch indices involved in the n operators S by

$$\mathbf{K} := (k_1, \dots, k_n), \quad \boldsymbol{\alpha} := (\alpha_1, \dots, \alpha_n), \quad \boldsymbol{\alpha}' := (\alpha'_1, \dots, \alpha'_n). \quad (37)$$

We are now in the position to write down the exact formula for n_q .

Theorem 1 (Main result, exact excitation density). *Let $q \in \mathbb{Z}^3$. If $q \in B_{\mathbb{F}}^c$, then the excitation density in the trial state $\psi = RT\Omega$ (11) from [2] is given by*

$$\begin{aligned} n_q = & \sum_{\substack{n=2 \\ n:\text{even}}}^{\infty} \frac{1}{2^n n!} \sum_{\mathbf{K}} \sum_{\boldsymbol{\alpha}, \boldsymbol{\alpha}'} \sum_{\substack{\mathbf{P}, \mathbf{P}' \\ \mathbf{H}, \mathbf{H}'}} \left(\prod_{j=1}^n \frac{\delta_{p_j, h_j \pm k_j} \delta_{p'_j, h'_j \pm k_j}}{n_{\alpha_j, k_j} n_{\alpha'_j, k_j}} K(k_j)_{\alpha_j, \alpha'_j} \right) \times \\ & \times \sum_{\xi \in \Xi_n} \sum_{(\pi_p, \pi_h) \in \Pi_n^{(\xi)}} \left(\prod_{p \in \mathbf{P}_- \cup \mathbf{P}'_-} \delta_{p, \pi_p(p)} \right) \left(\prod_{h \in \mathbf{H}_- \cup \mathbf{H}'_-} \delta_{h, \pi_h(h)} \right) \delta_{q, p_0} \delta_{q, p'_0} \text{sgn}(\xi, \pi_p, \pi_h), \end{aligned} \quad (38)$$

where the sum in \mathbf{K} runs over $(\Gamma^{\text{nor}})^n \subset \mathbb{Z}^{3n}$ (see (14)), the sums in $\boldsymbol{\alpha}, \boldsymbol{\alpha}'$ are such that $\alpha_j, \alpha'_j \in \mathcal{I}_{k_j}$ (see (12)), and the sums over $\mathbf{P}, \mathbf{P}', \mathbf{H}, \mathbf{H}'$ are such that $p_j, h_j : \alpha_j$ and $p'_j, h'_j : \alpha'_j$, that is,

$$\begin{aligned} p_j \in B_{\mathbb{F}}^c \cap B_{\alpha_j} \quad \text{and} \quad h_j \in B_{\mathbb{F}} \cap B_{\alpha_j} \quad \forall j \in \{1, \dots, n\}, \\ p'_j \in B_{\mathbb{F}}^c \cap B_{\alpha'_j} \quad \text{and} \quad h'_j \in B_{\mathbb{F}} \cap B_{\alpha'_j} \quad \forall j \in \{1, \dots, n\}. \end{aligned} \quad (39)$$

In case $q \in B_{\mathbb{F}}$, (38) remains valid after a replacement of $\delta_{q, p_0} \delta_{q, p'_0}$ by $\delta_{q, h_0} \delta_{q, h'_0}$.

The proof is given in Sect. 5 using Friedrichs diagrams. There, it will also become clear how the rather involved term in (38) arises from a step-by-step back-translation of Friedrichs diagrams into a mathematical expression.

Remark 1. *Convergence of the diagrammatic expansion.* The expansion (38) indeed converges: We obtain it by a separate evaluation of each order $n \in \mathbb{N}$ in the multicommutator expansion (26). Since the number of terms (i.e., diagrams) per order n is finite, the expansion (38) converges if and only if (26) converges. Now, $\|a_q^* a_q\| = 1$, so if we can show that S is bounded, then we obtain absolute convergence of the commutator series (26) as

$$\sum_{n=0}^{\infty} \frac{|\langle \Omega, \text{ad}_S^n(a_q^* a_q) \Omega \rangle|}{n!} \leq \sum_{n=0}^{\infty} \frac{\|\text{ad}_S^n(a_q^* a_q)\|}{n!} \leq \sum_{n=0}^{\infty} \frac{\|2S\|^n \|a_q^* a_q\|}{n!} = e^{\|2S\|}. \quad (40)$$

In fact, recalling (19) we have

$$\|S\| \leq \sum_{k \in \Gamma^{\text{nor}}} \sum_{\alpha, \beta \in \mathcal{I}_k} |K(k)_{\alpha, \beta}| \|c_{\alpha}^{\#}(k)\| \|c_{\beta}^{\#}(k)\|. \quad (41)$$

With [5, Lemma 7.1], we estimate $|K(k)_{\alpha, \beta}| \leq CM^{-1} \hat{V}(k)$. Further, by (16),

$$\|c_{\alpha}^*(k)\| \leq \frac{1}{n_{\alpha, k}} \sum_{\substack{p: p \in B_{\text{F}}^c \cap B_{\alpha} \\ p \mp k \in B_{\text{F}} \cap B_{\alpha}}} \|a_p^* a_{p \mp k}^*\| \leq \frac{1}{n_{\alpha, k}} \sum_{\substack{p: p \in B_{\text{F}}^c \cap B_{\alpha} \\ p \mp k \in B_{\text{F}} \cap B_{\alpha}}} 1 = n_{\alpha, k}, \quad (42)$$

and the same bound holds for $\|c_{\alpha}(k)\|$. With $n_{\alpha, k}^2 \leq CN^{\frac{2}{3}}M^{-1}$, which follows from the patch construction, and using that the sums $\sum_{\alpha}, \sum_{\beta}$ run over $\leq M$ elements, we conclude

$$\|2S\| \leq CM^{-1} \sum_{k \in \Gamma^{\text{nor}}} \hat{V}(k) \sum_{\alpha, \beta \in \mathcal{I}_k} n_{\alpha, k} n_{\beta, k} \leq CN^{\frac{2}{3}} \sum_{k \in \Gamma^{\text{nor}}} \hat{V}(k) < \infty, \quad (43)$$

since Γ^{nor} comprises finitely many lattice points.

Remark 2. *Allowed potentials and scaling limits.* In Theorem 1, we did not specify any conditions on V . Indeed, our result holds for *any potential* V , provided that $\hat{V} : \mathbb{Z}^3 \rightarrow \mathbb{R}$ exists. This may first seem somewhat surprising and is owed to the particular choice of the trial state ψ , involving finite sums $\sum_{k \in \Gamma^{\text{nor}}}$ in S (19), and \sum_p in $c_{\alpha}^{\#}(k)$ (16). However, if the potential $\hat{V}(k)$ does not satisfy the requirements of [5] that $\sum_{k \in \mathbb{Z}^3} \hat{V}(k) |k| < \infty$ and $\hat{V} \geq 0$, then there is no guarantee that ψ is a good approximation of the ground state (in terms of energy). So while Theorem 1 is still correct, its physical significance then still has to be demonstrated.

Likewise, we could pick any side length L of the torus and analogously construct a trial state ψ using the refined momentum lattice $\frac{2\pi}{L}\mathbb{Z}^3$. Then, sums will still be finite and Theorem 1 is still valid. In particular, Theorem 1 holds for any element of a sequence of trial states $(\psi_N)_{N \in \mathbb{N}}$, constructed as above, in *any scaling limit*, including the thermodynamic limit at high density ρ . However, there is no guarantee that these ψ_N will be good approximations for the ground state.

Remark 3. *Orders of the contributing diagrams.* As we explain in Sect. 6.1, the contractions $\delta_{p, \pi_p(p)}$ and $\delta_{h, \pi_h(h)}$ eliminate certain sums over α_j, α'_j by setting patch indices equal. As each sum runs over $\sim M$ elements, we expect the diagrams, indexed by (ξ, π_p, π_h) , to be of different orders, depending on how many sums survive. More precisely, we expect (38) to result in an expansion of the form

$$n_q = f_0 + f_1 M^{-1} + f_2 M^{-2} + f_3 M^{-3} + \dots, \quad (44)$$

where the coefficients $f_j \in \mathbb{R}$, $j \in \mathbb{N}$ have identical scaling in N . The leading order is expected to be $f_0 = n_q^{(b)}$, which scales like $\sim N^{-\frac{2}{3}}$ for “most” q , as explained in [1, Remark 2]. For the choice of the parameters M, δ as above [1, (10.53)], the optimal relative error of the approximation $n_q \approx n_q^{(b)}$ is thus expected to be $M^{-1} = N^{-\frac{10}{27}}$, which is much smaller than the existing relative error bound $N^{-\frac{2}{27}}$.

We believe that an expansion like (44) can be made rigorous, once suitable combinatorial bounds on the number of occurring diagrams have been derived.

We are able to interpret the bosonized excitation density $n_q^{(b)} \approx n_q$ obtained in [1, Thm. 3.1] as coming from a subset of bosonized Friedrichs diagrams, which we explain in Sect. 6. The subset is characterized by a restriction on (π_p, π_h) . First, we require that the two $c_\alpha^\sharp(k)$ -operators, whose momenta are contracted to $a_q^* a_q$, have their second momenta directly contracted to each other. Second, for all other $c_\alpha(k)$ -operators, both momenta must be contracted at the same time to some $c_\alpha^*(k)$ -operator. So in case $q \in B_F^c$, with $\sharp_1, \sharp_2 \in \{\cdot, '\}$ (so p^{\sharp_1} is either p or p'), the **bosonization constraint** reads

$$\begin{aligned} \pi_p^{-1}(p_0) = p_j^{\sharp_1} \quad \text{and} \quad \pi_p(p'_0) = p_\ell^{\sharp_2} &\Rightarrow \pi_h(h_j^{\sharp_1}) = h_\ell^{\sharp_2} \\ \forall j, \ell \geq 1 : \quad \pi_p(p_j^{\sharp_1}) = p_\ell^{\sharp_2} &\Rightarrow \pi_h(h_j^{\sharp_1}) = h_\ell^{\sharp_2}. \end{aligned} \quad (45)$$

The diagrammatic interpretation of this constraint is explained in Sect. 6.1 and depicted in Fig. 10. The restricted set of **bosonized contraction choices** is then

$$\Pi_{n,(b)}^{(\xi)} := \{(\pi_p, \pi_h) \in \Pi_n^{(\xi)} \mid (45) \text{ holds}\}. \quad (46)$$

Proposition 1 (Bosonized excitation density). *The bosonized excitation density $n_q^{(b)}$ (23) from [1] amounts to a restriction of (38) to bosonized diagrams, given by replacing $\Pi_n^{(\xi)}$ with $\Pi_{n,(b)}^{(\xi)}$. That is, for $q \in B_F^c$,*

$$\begin{aligned} n_q^{(b)} &= \sum_{\substack{n=2 \\ n:\text{even}}}^{\infty} \frac{1}{2^n n!} \sum_{\mathbf{K}} \sum_{\alpha, \alpha'} \sum_{\substack{\mathbf{P}, \mathbf{P}' \\ \mathbf{H}, \mathbf{H}'}} \left(\prod_{j=1}^n \frac{\delta_{p_j, h_j \pm k_j} \delta_{p'_j, h'_j \pm k_j}}{n_{\alpha_j, k_j} n_{\alpha'_j, k_j}} K(k_j)_{\alpha_j, \alpha'_j} \right) \times \\ &\times \sum_{\xi \in \Xi_n} \sum_{(\pi_p, \pi_h) \in \Pi_{n,(b)}^{(\xi)}} \left(\prod_{p \in \mathbf{P}_- \cup \mathbf{P}'_-} \delta_{p, \pi_p(p)} \right) \left(\prod_{h \in \mathbf{H}_- \cup \mathbf{H}'_-} \delta_{h, \pi_h(h)} \right) \delta_{q, p_0} \delta_{q, p'_0} \text{sgn}(\xi, \pi_p, \pi_h), \end{aligned} \quad (47)$$

and the same holds for $q \in B_F$ after a replacement of $\delta_{q, p_0} \delta_{q, p'_0}$ by $\delta_{q, h_0} \delta_{q, h'_0}$.

We illustrate and explain the meaning of (47) in Sect. 6.1 and give the diagrammatic proof of Proposition 1 in Sect. 6.2.

4 Friedrichs Diagram Formalism

Let us quickly recap the diagrammatic formalism by Friedrichs [18], for which we use the same notation as in [8]. Since we will need to evaluate both bosonic and fermionic commutators, we will assume in this section that a_q^*, a_q can describe both a species of fermionic or of bosonic creation/annihilation operators. That is, they satisfy either the CAR (9) or the CCR

$$[a_q, a_{q'}^*] = \delta_{q,q'}, \quad [a_q, a_{q'}] = [a_q^*, a_{q'}^*] = 0 \quad \text{for all } q, q' \in \mathbb{Z}^3. \quad (48)$$

In the formalism of Friedrichs diagrams, an operator of the form

$$A = \sum_{\substack{q_1, \dots, q_n \\ q'_1, \dots, q'_m}} f(q_1, \dots, q_n, q'_1, \dots, q'_m) a_{q_n}^* \dots a_{q_1}^* a_{q'_1} \dots a_{q'_m} \quad (49)$$

is represented by a vertex, see Fig. 3, that encodes the function (“kernel”) $f \in \ell^2(\mathbb{Z}^{3(n+m)})$ with n legs pointing to the left and m legs pointing to the right.



Figure 3: Left: A vertex with connectors, representing f and its momenta q_j, q'_j . Right: A Friedrichs diagram with one vertex, representing A in (49).

When taking multicommutators as in (26), the CCR/CAR will produce Kronecker deltas of the kind $\delta_{q,q'}$, which we represent by contracted legs. To be precise, a general Friedrichs diagram as in Fig. 4 consists of:

- V vertices, indexed by $v \in \{1, \dots, V\}$, representing $f_v : \mathbb{Z}^{3(n_v+m_v)} \rightarrow \mathbb{C}$.
- n_v left-connectors and m_v right-connectors on each vertex, representing the momenta $q_{v,1}, \dots, q_{v,n_v}$ and $q'_{v,1}, \dots, q'_{v,m_v}$, respectively. So the total index sets are

$$\begin{aligned} \mathcal{J} &= \bigcup_{v=1}^V \mathcal{J}_v, & \mathcal{J}_v &:= \{(v, 1), \dots, (v, n_v)\} & \text{and} \\ \mathcal{J}' &= \bigcup_{v=1}^V \mathcal{J}'_v, & \mathcal{J}'_v &:= \{(v, 1), \dots, (v, m_v)\}. \end{aligned} \quad (50)$$

- $C \leq \min\{|\mathcal{J}|, |\mathcal{J}'|\}$ contractions between a left- and a right-connector. We formally keep track of them by two maps³ $\pi : \{1, \dots, C\} \rightarrow \mathcal{J}$ and $\pi' : \{1, \dots, C\} \rightarrow \mathcal{J}'$, where a contraction goes from connector $\pi'(c)$ to $\pi(c)$.

³We remark that π, π' do not play the same role as π_p, π_h above. Here, π indexes contracted

- $|\mathcal{J}| + |\mathcal{J}'| - 2C$ external legs, one for each uncontracted connector, representing creation operators a_q^* (for left-connectors) or annihilation operators $a_{q'}$ (for right-connectors). We formally keep track of the operator orderings by maps $\sigma : \{1, \dots, |\mathcal{J}| - C\} \rightarrow \mathcal{J}$ and $\sigma' : \{1, \dots, |\mathcal{J}'| - C\} \rightarrow \mathcal{J}'$

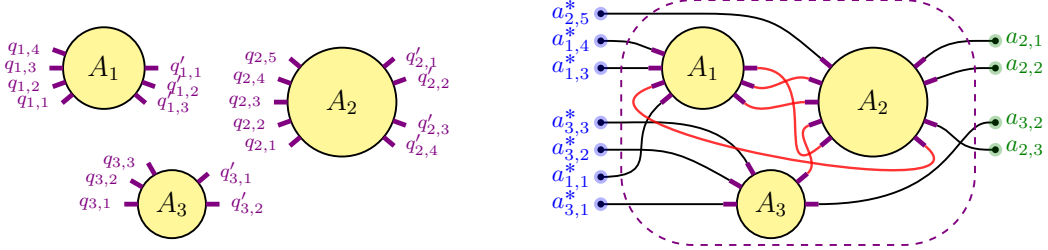


Figure 4: Left: Vertices and connectors of a Friedrichs diagram with 3 vertices. Right: A Friedrichs diagram with 3 vertices.

For brevity, we introduce the momentum vectors $\mathbf{Q}_v := (q_{v,1}, \dots, q_{v,n_v})$, $\mathbf{Q}'_v := (q'_{v,1}, \dots, q'_{v,m_v})$ and $\mathbf{Q} = (\mathbf{Q}_1, \dots, \mathbf{Q}_V)$, $\mathbf{Q}' = (\mathbf{Q}'_1, \dots, \mathbf{Q}'_V)$ and abbreviate $a_{q_{v,\ell}}^* := a_{v,\ell}^*$ and $a_{q'_{v,\ell}} := a_{v,\ell}$. A Friedrichs diagram can then be translated into an operator

$$G = \sum_{\mathbf{Q}, \mathbf{Q}'} \left(\prod_{v=1}^V f_v(\mathbf{Q}_v, \mathbf{Q}'_v) \right) \left(\prod_{c=1}^C \delta_{q_{\pi(c)}, q'_{\pi'(c)}} \right) \left(\prod_{\ell=1}^{|\mathcal{J}|-C} a_{\sigma(\ell)} \right)^* \left(\prod_{\ell'=1}^{|\mathcal{J}'|-C} a_{\sigma'(\ell')} \right). \quad (51)$$

Note that (51) is again an operator of the form (49), so it can alternatively be written as a Friedrichs diagram with a single vertex.

Commutators between two bosonic or two fermionic operators A_1 and A_2 of type (49) can now be expressed in terms of so-called attached products $A_1 \text{---} A_2$ (bosonic) and $A_1 \text{---} A_2$ (fermionic): Loosely speaking, those are “sums over all ways to contract A_1 with A_2 from left to right”, possibly including signs. Mathematically, we may track the “ways to contract” by the set of contraction configurations

$$\mathcal{C} := \left\{ (\pi, \pi') \mid \pi : \{1, \dots, C\} \rightarrow \mathcal{J}_2, \pi' : \{1, \dots, C\} \rightarrow \mathcal{J}'_1, \right. \\ \left. 1 \leq C \leq \min(m_1, n_2), |\text{imag}(\pi')| = C, \pi(1) > \dots > \pi(C) \right\}, \quad (52)$$

where each (π, π') renders two sets of contractible but uncontracted connectors

$$\mathcal{U} := \left\{ (2, j) \in \mathcal{J}_2 \mid \nexists c \in \{1, \dots, C\} : \pi(c) = (2, j) \right\}, \\ \mathcal{U}' := \left\{ (1, k) \in \mathcal{J}'_1 \mid \nexists c \in \{1, \dots, C\} : \pi'(c) = (1, k) \right\}. \quad (53)$$

connectors on the left and π' those on the right, while π_p, π_h directly associate connectors on the left to those on the right. In fact, the notation with π, π' is more general. Above, we chose the more compact notation with π_p, π_h , since there we are in a special case where we know that all connectors have to be contracted.



Figure 5: Left: A maximally crossed Friedrichs diagram.

Right: In this diagram, a permutation σ' with 3 swaps is necessary to achieve a maximally crossed form. So $\text{sgn}(\sigma') = -1$.

The **bosonic attached product** is then defined as

$$\begin{aligned}
A_1 \text{---} \circ \text{---} A_2 := & \sum_{(\pi, \pi') \in \mathcal{C}} \sum_{\mathbf{Q}, \mathbf{Q}'} f_1(\mathbf{Q}_1, \mathbf{Q}'_1) f_2(\mathbf{Q}_2, \mathbf{Q}'_2) \left(\prod_{c=1}^C \delta_{q_{\pi(c)}, q'_{\pi'(c)}} \right) \times \\
& \times \left(\prod_{\ell=1}^{n_1} a_{1,\ell} \right)^* \left(\prod_{u \in \mathcal{U}} a_u \right)^* \prod_{u' \in \mathcal{U}'} a_{u'} \prod_{\ell'=1}^{m_2} a_{2,\ell'} .
\end{aligned} \tag{54}$$

For fermions, the attached product is defined analogously, up to a change of sign in front of certain contributions: Let σ, σ' be the permutations of \mathcal{J}_2 and \mathcal{J}'_1 that take the diagram into a **maximally crossed** form, while preserving the order of the uncontracted connectors. Here, by maximally crossed, we mean that the first right-connector of A_1 from the bottom, $(1, m_1)$, is connected to the first left-connector of A_2 from the top, $(2, n_2)$, the second to the second, and so on. That means,

$$\begin{aligned}
\sigma(\pi(c)) &= (2, n_2 - c + 1) & \text{and} & & u_1 < u_2 \Rightarrow \sigma(u_1) < \sigma(u_2) & & \forall u_1, u_2 \in \mathcal{U} , \\
\sigma(\pi'(c)) &= (1, m_1 - c + 1) & \text{and} & & u'_1 < u'_2 \Rightarrow \sigma'(u'_1) < \sigma'(u'_2) & & \forall u'_1, u'_2 \in \mathcal{U}' .
\end{aligned} \tag{55}$$

See also Fig. 5. The sign of a contraction configuration $(\pi, \pi') \in \mathcal{C}$ is then given by

$$\text{sgn}(\pi, \pi') := (-1)^{(m_1 - C)(n_2 - C)} \text{sgn}(\sigma) \text{sgn}(\sigma') \tag{56}$$

and the **fermionic attached product** is defined as

$$\begin{aligned}
A_1 \text{---} \circ \text{---} A_2 := & \sum_{(\pi, \pi') \in \mathcal{C}} \text{sgn}(\pi, \pi') \sum_{\mathbf{Q}, \mathbf{Q}'} f_1(\mathbf{Q}_1, \mathbf{Q}'_1) f_2(\mathbf{Q}_2, \mathbf{Q}'_2) \prod_{c=1}^C \delta_{q_{\pi(c)}, q'_{\pi'(c)}} \times \\
& \times \left(\prod_{\ell=1}^{n_1} a_{1,\ell} \right)^* \left(\prod_{u \in \mathcal{U}} a_u \right)^* \prod_{u' \in \mathcal{U}'} a_{u'} \prod_{\ell'=1}^{m_2} a_{2,\ell'} .
\end{aligned} \tag{57}$$

For a motivation of the sign factor $\text{sgn}(\pi, \pi')$, see [8, Appendix A].

(Anti-)commutators can now conveniently be expressed in terms of attached products.

Proposition 2 ([8, Theorems 3.1 and 3.2]). *For bosonic operators of the form (49), we have*

$$[A_1, A_2] = A_1 \text{--}\circ\text{--}A_2 - A_2 \text{--}\circ\text{--}A_1 . \quad (58)$$

For fermionic operators of the form (49), we have

$$\begin{aligned} [A_1, A_2] &= A_1 \text{--}\circ\text{--}A_2 - A_2 \text{--}\circ\text{--}A_1 && \text{if } (m_1 n_2 + m_2 n_1) \text{ is even ,} \\ \{A_1, A_2\} &= A_1 \text{--}\circ\text{--}A_2 + A_2 \text{--}\circ\text{--}A_1 && \text{if } (m_1 n_2 + m_2 n_1) \text{ is odd .} \end{aligned} \quad (59)$$

With these commutator formulas at hand, we are ready to evaluate the multicommutator in (26) diagrammatically.

5 Multicommutator Evaluation via Friedrichs Diagrams

Using Friedrichs diagrams, we will now evaluate the multicommutator in (26) to derive the formula (38) for n_q as claimed in Theorem 1.

Proof of Theorem 1. Recall (26):

$$n_q = \sum_{n=0}^{\infty} \frac{1}{n!} \langle \Omega, \text{ad}_S^n(a_q^* a_q) \Omega \rangle .$$

First, let us specify how to represent the operators $a_q^* a_q$, $c_\alpha^*(k)$, $c_\alpha(k)$, and S diagrammatically, see Fig. 6.

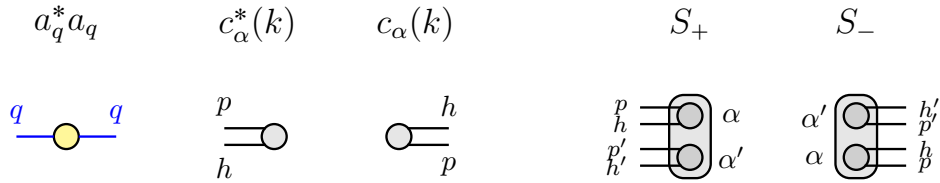


Figure 6: From left to right: The operators $a_q^* a_q$, $c_\alpha^*(k)$, $c_\alpha(k)$ and $S = S_+ + S_-$ are translated into Friedrichs diagrams.

- The operator $a_q^* a_q$ is characterized by the kernel $f(p_0, p'_0) = \delta_{q, p_0} \delta_{q, p'_0}$ in case $q \in B_F^c$ and $f(h_0, h'_0) = \delta_{q, h_0} \delta_{q, h'_0}$ if $q \in B_F$. We represent it by a small vertex.

- Each operator $c_\alpha^*(k)$ is characterized by a kernel

$$f(p, h) = d_{\alpha, k}(p, h) := \delta_{p, h \pm k} \frac{1}{n_{\alpha, k}} \chi_{B_{\mathbb{F}}^c \cap B_\alpha}(p) \chi_{B_{\mathbb{F}} \cap B_\alpha}(h) , \quad (60)$$

compare (16), where we adopted the notation of [1, (4.2) and (4.1)]. We also represent $c_\alpha^*(k)$ by a small vertex, whose two legs are pointing left.

- Likewise, $c_\alpha(k)$ is represented by a small vertex with two legs pointing to the right. The directions in which the legs are pointing makes it clear, which operator is meant by which small vertex.
- We represent the creation part S_+ of S by a large rectangular vertex including two smaller c^* -vertices. The large vertex can then be translated into a factor of $\frac{1}{2}K(k)_{\alpha, \alpha'}$, where sums over k, α , and α' are implicitly assumed. Further, the large vertex fixes both momentum transfers inside the small vertices $c_\alpha^*(k)$ and $c_{\alpha'}^*(k)$ to be the same vector $k \in \Gamma^{\text{nor}} \subset \mathbb{Z}^3$.

Likewise, S_- is represented by a large vertex with 4 legs pointing to the right.

We would like to apply Proposition 2 for evaluating the multicommutators $\text{ad}_S^n(a_q^* a_q)$ in (26). In each commutator $\text{ad}_S^n(a_q^* a_q) = [S_+, \text{ad}_S^{n-1}(a_q^* a_q)] + [S_-, \text{ad}_S^{n-1}(a_q^* a_q)]$, the leg numbers of the first vertex $A_1 := S_\pm$ are $(n_1, m_1) = (4, 0)$ or $(0, 4)$, respectively. So irrespective of the leg numbers of the diagrams in $A_2 := \text{ad}_S^{n-1}(a_q^* a_q)$, we have $m_1 n_2 + n_1 m_2 = 4n_2$ or $m_1 n_2 + n_1 m_2 = 4m_2$, which are both even. Thus, (59) indeed renders a formula for a commutator.

Now, following Proposition 2, the multicommutators $\text{ad}_S^n(a_q^* a_q)$ in (26) correspond to diagrams, which are built by starting with an $a_q^* a_q$ -vertex and successively contracting n vertices of type S_\pm into the diagram.

After taking the vacuum expectation value $\langle \Omega, \text{ad}_S^n(a_q^* a_q) \Omega \rangle$, any diagram with external legs will vanish as it yields linear combinations of terms of the form $\langle \Omega, a_{q_n}^* \dots a_{q_1}^* a_{q_1'} \dots a_{q_m'} \Omega \rangle$, and we have $a_q \Omega = 0$. So we only need to consider diagrams where all $4n + 2$ legs have been contracted. As contractions always connect a left- and a right-connector, we need to have $2n + 1$ connectors of either kind. So only diagrams with $\frac{n}{2}$ vertices of type S_+ and $\frac{n}{2}$ vertices of type S_- contribute. In particular,

$$\langle \Omega, \text{ad}_S^n(a_q^* a_q) \Omega \rangle = 0 \quad \text{if } n \text{ is odd} , \quad (61)$$

and the sum in (26) reduces to even n .

In order to derive (38), let us back-translate the corresponding diagrams. Irrespective of the contractions, the S -vertices contribute the sums $\sum_{K \in (\Gamma^{\text{nor}})^n}$ and $\sum_{\alpha, \alpha'}$, see (37), such that $\alpha_j, \alpha'_j \in \mathcal{I}_{k_j}$, as claimed in Theorem 1.

The $4n + 2$ momenta of the connectors are tracked in $\mathbf{P}, \mathbf{P}', \mathbf{H}, \mathbf{H}'$, see (28), where the

condition (39) encodes the factors $\chi_{B_{\mathbb{F}}^c \cap B_\alpha}(p)$ and $\chi_{B_{\mathbb{F}} \cap B_\alpha}(h)$ from the $c_\alpha^\sharp(k)$ -vertices. Now, for $1 \leq j \leq n$, every S_- -vertex also contributes a factor of $\frac{1}{2}K(k_j)_{\alpha_j, \alpha'_j}$ and every S_+ -vertex a factor of $-\frac{1}{2}K(k_j)_{\alpha_j, \alpha'_j}$. As S_+ contains creation operators, it gets contracted “from the right”, yielding a contribution $\text{ad}_S^{j-1}(a_q^* a_q) \text{--} \circ \text{--} S_+$ which comes with an additional minus sign, see (59). So including the sign from (59), both S_+ and S_- effectively contribute $\frac{1}{2}K(k_j)_{\alpha_j, \alpha'_j}$. Further, the two $c_\alpha^\sharp(k)$ -vertices in S_\pm contribute a factor of $\delta_{p_j, h_j \pm k_j} n_{\alpha_j, k_j}^{-1}$ and $\delta_{p'_j, h'_j \pm k_j} n_{\alpha'_j, k_j}^{-1}$. Recalling that each order $n \in \mathbb{N}$ comes with a factor of $(n!)^{-1}$ in the series (26), this reproduces the first line of (38).

The second line of (38) now accounts for contractions in the diagrams. As explained around (29), the map $\xi \in \Xi_n$ tracks whether S_+ or S_- has been chosen for contraction, which is unique for each diagram.

Accordingly, we split the connectors into those on the right $(\mathbf{P}_+, \mathbf{P}'_+, \mathbf{H}_+, \mathbf{H}'_+)$, and those on the left $(\mathbf{P}_-, \mathbf{P}'_-, \mathbf{H}_-, \mathbf{H}'_-)$ as in (30).

The $2n + 1$ contractions are tracked by the bijective maps π_p, π_h as in (31). Here, π_p associates to every particle-connector p on the left a particle-connector $\pi_p(p)$ on the right to which p is contracted. Every such contraction results in a contribution of $\delta_{p, \pi_p(p)}$. Likewise, every hole-connector h on the left is contracted to $\pi_h(h)$ on the right, resulting in a contribution of $\delta_{h, \pi_h(h)}$.

As the attached product $\text{--} \circ \text{--}$ must include at least one contraction, we require the j -th S -vertex to be contracted to an existing ℓ -th vertex ($\ell < j$). This is exactly constraint (32), resulting in the contraction sum running over $(\pi_p, \pi_h) \in \Pi_n^{(\xi)}$.

Finally, the factor of $\delta_{q, p_0} \delta_{q, p'_0}$ or $\delta_{q, h_0} \delta_{q, h'_0}$ is just the kernel of the $a_q^* a_q$ -vertex, as explained above.

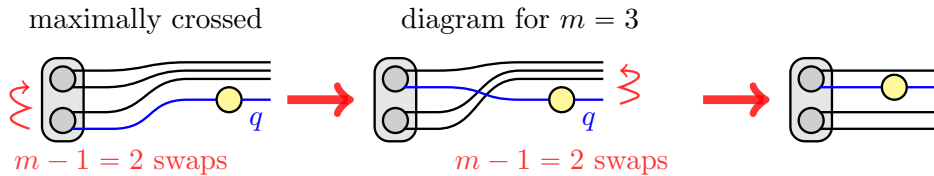


Figure 7: After the first contraction, the diagram can be brought into the same structure as S_\pm , while picking up a sign factor of $(-1)^{2m-2} = 1$.

The only remaining step is to evaluate the sign factors $\text{sgn}(\pi, \pi')$ as in (56) and to show that their product amounts to the factor $\text{sgn}(\xi, \pi_p, \pi_h)$ in (36). We start with considering the first contraction, which appears in $\text{ad}_S^1(a_q^* a_q) = [S_+, a_q^* a_q] + [S_-, a_q^* a_q]$. Here, one q -connector gets contracted to any of the 4 connectors of S_\pm , say, the m -th one, counted from the top for S_+ and from the bottom for S_- . The diagram then arises from a maximally crossed one by employing $m - 1$ swaps, see Fig. 7. If we now swap the

remaining uncontracted a_q^\sharp -operator into the position, where the contracted operator of S_\pm used to be (second step in Fig. 7), we have to apply further $m - 1$ swaps. After this move, we end up with an operator that has the same structure as an S_\pm -operator, while the sign factor we pick up is $(-1)^{2m-2} = 1$. So for the sign evaluation, we can proceed as if the $a_q^*a_q$ -vertex didn't exist.

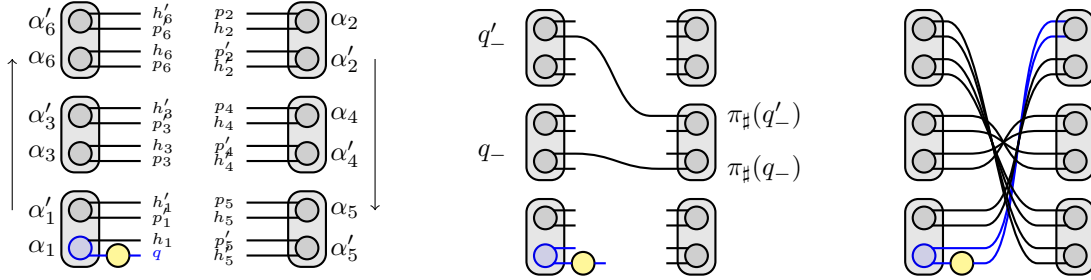


Figure 8: Left: Example of a diagram with $n = 6$ vertices where only the first contraction drawn.

Middle: A situation with $q'_- > q_-$ and $\pi_\sharp(q'_-) < \pi_\sharp(q_-)$, making a swap necessary to finally achieve maximal crossing.

Right: A maximally crossed diagram with $n = 6$.

In the following contraction steps, we then successively add S_- -diagrams from the bottom to the top on the left-hand side and S_+ -diagrams from the top to the bottom on the right-hand side, see Fig. 8. Note that the order (bottom to top or vice versa) is enforced by the ordering prescription introduced in (49) and below. Also, observe that the ordering relation $q'_- > q_-$ in (35) and (36) just means that the connector q'_- is above q_- in the diagram, while $\pi_\sharp(q'_-) < \pi_\sharp(q_-)$ means that the connector $\pi_\sharp(q'_-)$ is above $\pi_\sharp(q_-)$, see also Fig. 8. So the sign factor $\text{sgn}(\xi, \pi_p, \pi_h)$ in (36) essentially counts how many swaps would be necessary to take the diagram into maximally crossed form⁴ as depicted in Fig. 8, while ignoring the $a_q^*a_q$ -vertex. Thus, we may finish the proof by establishing the following claim.

Claim: The product of all sign factors $\text{sgn}(\pi, \pi')$ appearing in the multicommutator evaluation for every diagram indexed by (ξ, π_p, π_h) is identical to the sign factor $\text{sgn}(\xi, \pi_p, \pi_h)$ we would need to make the diagram, including n vertices S_\pm and ignoring $a_q^*a_q$, maximally crossed.

Proof of the Claim: Following (56), a factor of (-1) in $\text{sgn}(\pi, \pi')$ enters if and only if within the contraction of a new S_\pm -vertex:

⁴Note that the maximally crossed diagram in Fig. 8 does not contribute to n_q due to the constraint (32).

- (A) A connector gets contracted, and it has to be swapped with another connector in order to achieve maximal crossing. This rule accounts for the factor of $\text{sgn}(\sigma)\text{sgn}(\sigma')$ in (56).
- (B) A connector of some operator a is not contracted and has to “jump” over another uncontracted operator a^* to achieve normal ordering. This accounts for $(-1)^{(m_1-C)(n_2-C)}$ in (56).

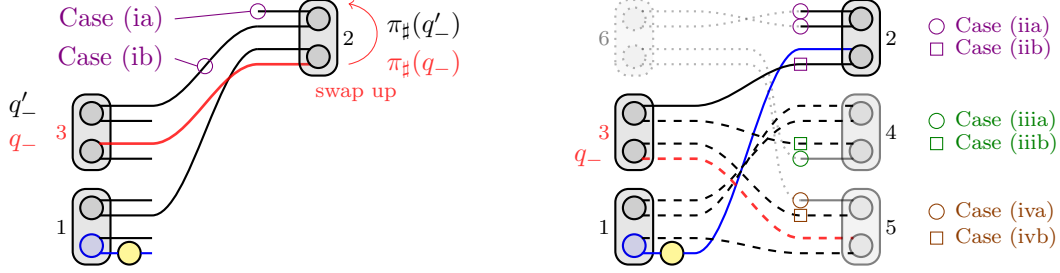


Figure 9: Left: Cases (ia) and (ib), in which q_- is accounted for a factor of (-1) . Right: Cases (ii), (iii) and (iv). The numbers 1–6 indicate the order in which S_{\pm} -vertices enter the diagram. Here, $j = 3$.

We now re-distribute the sign factors (-1) coming from (A) and (B) among the $2n$ connectors on the left-hand side, $q_- \in \{p_j, p'_j, h_j, h'_j\} \subset \mathbf{Q}_-$, by making every q_- accountable for the following factors of (-1) , see Fig. 9:

- (i) If q_- gets contracted to $\pi_{\#}(q_-)$ immediately as the j -th vertex $S_{\pm} = S_-$ enters, we make it accountable for all (-1) of type (A) caused by $\pi_{\#}(q_-)$ being swapped upwards past all connectors above $\pi_{\#}(q_-)$ that are
- (ia) uncontracted or
 - (ib) contracted to some connector q'_- above q_- .
- (ii) If q_- does not immediately get contracted as the j -th vertex $S_{\pm} = S_-$ enters, we make it accountable for
- (iia) all (-1) of type (B) caused by q_- jumping over uncontracted connectors on the right and
 - (iib) all (-1) of type (A) caused by connectors $q'_- > q_-$ being swapped down below q_- .
- (iii) As an ℓ -th vertex $S_{\pm} = S_+$, $\ell > j$ enters, and q_- is still not contracted, we make it accountable for
- (iiia) all (-1) of type (B) caused by q_- jumping over uncontracted connectors in S_- and

- (iiib) all (-1) of type (A) caused by connectors $q'_- > q_-$ that got contracted to vertex ℓ and have to be swapped down past q_- .
- (iv) As an ℓ -th vertex $S_{\pm} = S_+, \ell > j$ enters, and q_- is contracted to $\pi_{\#}(q_-)$ within this step, we make q_- accountable for $\pi_{\#}(q_-)$ being swapped past
 - (iva) all uncontracted connectors in the ℓ -th S_{\pm} above $\pi_{\#}(q_-)$
 - (ivb) all connectors in the ℓ -th S_{\pm} above $\pi_{\#}(q_-)$ contracted to some $q'_- > q_-$.

Indeed, multiplying all sign factors (-1) from (i)–(iv) for all q_- recovers exactly contributions (A) and (B): It is easy to see that, as the j -th S -vertex enters, and it is of type S_- , then the contributions (iia) from all uncontracted q_- in this S_- make up all sign factors of type (B) occurring in this step. Further, (ia) and (ib) account for all swaps on the right and (iib) for all swaps on the left that are needed to achieve maximal crossing in this step, rendering all sign factors of (A).

By contrast, if an S_+ -vertex enters, then (iiia) will yield all sign factors of type (B) in this step. Then, (iiib) accounts for all swaps on the left, and (iva) and (ivb) for all swaps on the right that yield maximal crossing after the step, rendering the factors (A). So all factors (i)–(iv) from all q_- indeed render the total product of all sign factors $\text{sgn}(\pi, \pi')$ appearing in the n contractions.

Now, let us determine the sign factor $\text{sgn}(\xi, \pi_p, \pi_h)$ appearing when swapping the entire diagram into maximally crossed form, as in Fig. 8. The transition to maximal crossing can be achieved by successively considering connectors $q_- \in \mathbf{Q}_-$ and swapping $\pi_{\#}(q_-)$ on the right past all $\pi_{\#}(q'_-) < \pi_{\#}(q_-)$ with $q'_- > q_-$.

First, assume that q_- is contracted immediately as the j -th vertex S_{\pm} enters. Any $q'_- > q_-$ with $\pi_{\#}(q'_-) < \pi_{\#}(q_-)$ is either in the j -th vertex, rendering (ib), or above the j -th vertex, so $\pi_{\#}(q'_-)$ is not yet contracted in step j , rendering (ia).

Conversely, assume that q_- is not immediately contracted as the j -th vertex S_{\pm} enters, but only in step $\ell > j$. Then, for the connectors $\pi_{\#}(q'_-)$ swapped with $\pi_{\#}(q_-)$ there are the following options: $\pi_{\#}(q'_-)$ could be present in the diagram after step j and at this point either already contracted to some $q'_- > q_-$, rendering (iib), or uncontracted, so it gets later contracted to q'_- in some S_- -vertex above q_- , rendering contribution (iia). Or, $\pi_{\#}(q'_-)$ could join the diagram in steps $j+1$ through ℓ , rendering contributions (iiib) and (ivb) if it is immediately contracted to some $q'_- > q_-$, or contributions (iiia) and (iva) if it is yet uncontracted upon entering and gets later contracted to a q'_- in some vertex above the j -th. After step ℓ , only connectors $\pi_{\#}(q'_-)$ below $\pi_{\#}(q_-)$ enter, which do not contribute to the swaps encoded in (36).

Concluding both cases, we observe that multiplying all sign factors (i)–(iv) for all q_- also renders exactly the factor needed to swap the entire diagram into maximally crossed form, viz. $\text{sgn}(\xi, \pi_p, \pi_h)$. This establishes the claim and concludes the proof.

□

6 Bosonization Approximation in Friedrichs Diagrams

Formula (38) is rather bulky, as it contains many contributions of various forms. Therefore, it makes sense to restrict to those Friedrichs diagrams, which we expect to make the largest contribution. These are exactly the diagrams corresponding to the bosonization approximation in [1], as we will see in this section.

6.1 Heuristic Motivation

To get a heuristic intuition of which diagrams make the largest contribution, consider the first two Friedrichs diagrams in Fig. 10, which both contribute to $\langle \Omega, \text{ad}^6 S(a_q^* a_q) \Omega \rangle$. As a contraction $\delta_{q_-, \pi_{\sharp}(q_-)}$ sets the momenta of the two adjacent connectors q_- and $\pi_{\sharp}(q_-)$ equal, it also sets the patch index of the corresponding c^{\sharp} -vertices equal to some α_j . The set of c^{\sharp} -vertices thus decays into subsets of size ≥ 2 with identical patch indices. In each subset of m c^{\sharp} -vertices, the m adjacent contractions form a single loop that successively runs through all vertices. For instance, the first diagram in Fig. 10 contains 3 loops, which run through $m = 6, 4$ and 2 c^{\sharp} -vertices, respectively. The loop with 6 c^{\sharp} -vertices also runs through $a_q^* a_q$, so its patch index is fixed to α_q . The two shorter loops carry patch indices α_1 and α_2 , over which we have to take a double sum $\sum_{\alpha_1, \alpha_2}$.

As each sum \sum_{α_j} contains $\sim M$ terms, we expect the largest contributions to come from diagrams with the largest loop number. This is achieved if all loops⁵ have length 2, resulting in n loops, as depicted in the second diagram in Fig. 10. The diagrammatic contribution then contains an $(n - 1)$ -fold sum $\sum_{\alpha_1, \dots, \alpha_{n-1}}$. In that case, the two contractions in each loop (except the one running through the $a_q^* a_q$ -vertex) form a pair and effectively act like a single bosonic contraction, as depicted in the third diagram in Fig. 10.

We can thus think of the restriction to diagrams where only loops of length 2 are permitted as some kind of bosonization. These diagrams turn out to be particularly easy to evaluate and are expected to give the largest contribution to n_q .

6.2 Evaluating the Bosonized Multicommutator Diagrammatically

Proof of Proposition 1. We directly evaluate the right-hand side of (47) diagrammatically and show that it amounts to the cosh-term in (23). First, notice that the constraint (45), in the language of the previous subsection, exactly means that we restrict to bosonized diagrams with only loops including 2 c^{\sharp} -vertices. Thus, the right-hand side

⁵The length of a loop refers to the number of c^{\sharp} -vertices it runs through, not taking into consideration $a_q^* a_q$.

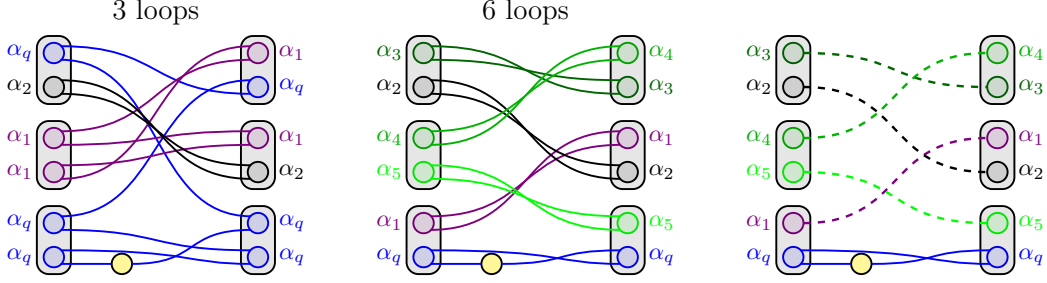


Figure 10: Left: A generic Friedrichs diagram with 3 loops of lengths 6, 4, and 2. Middle: A Friedrichs diagram with maximal number of loops 6, all of length 2. Right: Bosonization—fermionic contraction pairs have been replaced by bosonic contractions.

of (47) is just a sum over all bosonized diagrams.

Let us evaluate these diagrams (compare also Fig. 10). First, note that there are n loops, where in each loop, the contractions set the adjacent patch indices equal. The patch index of the loop involving the $a_q^* a_q$ -vertex is fixed to α_q . So the patch index sum $\sum_{\alpha, \alpha'}$ reduces to a sum over $n - 1$ loops, namely those in $\alpha \setminus \alpha_j$. The contractions in a loop also set all momentum transfers k_j of the adjacent S_{\pm} -vertices equal. Now observe that all bosonized diagrams are fully connected, since otherwise constraint (32) is violated. Thus, all k_j are set equal to one single momentum transfer $k \in \Gamma^{\text{nor}}$ and the n -fold sum $\sum_{\mathbf{K}}$ reduces to a single sum \sum_k . The contributing K -matrix elements then become $K(k)_{\alpha_j, \beta(\alpha_j)}$ with $\beta : \alpha \rightarrow \alpha$ being an appropriate cyclic permutation.

Further, by the bosonization assumption (45), $p_j^{\sharp} = \pi_p(p_j^{\sharp})$ already implies $h_j^{\sharp} = \pi_h(h_j^{\sharp})$ so the product $\prod_{h \in \mathbf{H} \cup \mathbf{H}'} \delta_{h, \pi_h(h)}$ in (47) becomes redundant and can be eliminated. Also, the factor $\delta_{p_j, h_j \pm k_j} \delta_{p'_j, h'_j \pm k_j} = \delta_{p_j, h_j \pm k} \delta_{p'_j, h'_j \pm k}$ in (47) eliminates the sums over \mathbf{H}, \mathbf{H}' , while leaving the condition that $h_j = p_j \mp k$ and $h'_j = p'_j \mp k$ be holes in patch α_j . Let us denote these conditions as

$$\chi(\mathbf{H}, \mathbf{H}' : \alpha) := \prod_{j=1}^n \chi(h_j, h'_j : \alpha_j) = \prod_{j=1}^n \chi(p_j \mp k \in B_{\alpha_j} \cap B_{\mathbf{F}}) \chi(p'_j \mp k \in B_{\alpha_j} \cap B_{\mathbf{F}}). \quad (62)$$

So the r.h.s. of (47) becomes

$$\begin{aligned} \text{r.h.s.} &= \sum_{\substack{n=2 \\ n:\text{even}}}^{\infty} \frac{1}{2^n n!} \sum_{\xi \in \Xi_n} \sum_{(\pi_p, \pi_h) \in \Pi_{n, (b)}^{(\xi)}} \sum_k \sum_{\alpha \setminus \alpha_q} \sum_{\mathbf{P}, \mathbf{P}'} \chi(\mathbf{H}, \mathbf{H}' : \alpha) \times \\ &\times \left(\prod_{p \in \mathbf{P}_- \cup \mathbf{P}'_-} \delta_{p, \pi_p(p)} \right) \left(\prod_{j=1}^n \frac{1}{n_{\alpha_j, k}^2} K(k)_{\alpha_j, \beta(\alpha_j)} \right) \delta_{q, p_0} \delta_{q, p'_0} \text{sgn}(\xi, \pi_p, \pi_h). \end{aligned} \quad (63)$$

Now, the contractions $\delta_{p, \pi_p(p)}$, not involving p_0 , eliminate the sums in \mathbf{P}, \mathbf{P}' over all connectors on the right, that is, over all momentum indices $p_j \in \mathbf{P}_+ \setminus p_0$ and $p'_j \in \mathbf{P}'_+$,

or equivalently, all p_j, p'_j with $\xi(j) = 1$. So only those p_j, p'_j on the left ($\xi(j) = -1$) and p_0, p'_0 survive. The condition $h_j, h'_j : \alpha_j$ is then automatically fulfilled for all j with $\xi(j) = 1$, so we only need to impose it on those j with $\xi(j) = -1$:

$$\begin{aligned} & \sum_{\mathbf{P}, \mathbf{P}'} \chi(\bar{\mathbf{H}}, \mathbf{H}' : \boldsymbol{\alpha}) \left(\prod_{p \in \mathbf{P}_- \cup \mathbf{P}'_-} \delta_{p, \pi_p(p)} \right) \delta_{q, p_0} \delta_{q, p'_0} \\ &= \sum_{p_0, p'_0} \left(\prod_{j: \xi(j) = -1} \sum_{p_j, p'_j} \chi(h_j, h'_j : \alpha_j) \right) \delta_{\pi_p^{-1}(p_0), p_0} \delta_{q, p_0} \delta_{q, p'_0}. \end{aligned} \quad (64)$$

The sums \sum_{p_j, p'_j} run over all particle-hole pairs and thus amount to $n_{\alpha_j, k}^2$, except for the sum over $\pi_p^{-1}(p_0)$, which is eliminated by $\delta_{\pi_p^{-1}(p_0), p_0} \delta_{q, p_0}$. Now observe that every loop with unique patch index α_j contains exactly one index p_j or p'_j on the left ($\xi(j) = -1$). So we get exactly one factor $n_{\alpha_j, k}^2$ for every α_j , except for $n_{\alpha_q, k}^2$. Thus,

$$\text{r.h.s.} = \sum_{\substack{n=2 \\ n:\text{even}}}^{\infty} \frac{1}{2^n n!} \sum_{\xi} \sum_{(\pi_p, \pi_h)} \sum_k \frac{1}{n_{\alpha_q, k}^2} \sum_{\boldsymbol{\alpha} \setminus \alpha_q} \left(\prod_{j=1}^n K(k)_{\alpha_j, \beta(\alpha_j)} \right) \text{sgn}(\xi, \pi_p, \pi_h). \quad (65)$$

Note that the sum over $k \in \Gamma^{\text{nor}}$ here gets reduced to those k with $\alpha_q \in \mathcal{I}_k$ and $q \mp k : \alpha_q$, as otherwise, the contribution vanishes. So comparing with (25), the sum becomes $\sum_k = \sum_{k \in \tilde{\mathcal{C}}^q \cap \mathbb{Z}^3}$. As β is cyclic, the sum in $\boldsymbol{\alpha} \setminus \alpha_j$ over the K -matrix elements amounts to an $(n-1)$ -fold matrix multiplication, so

$$\text{r.h.s.} = \sum_{\substack{n=2 \\ n:\text{even}}}^{\infty} \frac{1}{2^n n!} \sum_{\xi} \sum_{(\pi_p, \pi_h)} \sum_{k \in \tilde{\mathcal{C}}^q \cap \mathbb{Z}^3} \frac{1}{n_{\alpha_q, k}^2} (K(k)^n)_{\alpha_q, \alpha_q} \text{sgn}(\xi, \pi_p, \pi_h). \quad (66)$$

Next, we evaluate the sign factor $\text{sgn}(\xi, \pi_p, \pi_h)$, which is the same one needed to bring the entire diagram into maximally crossed form while ignoring $a_q^* a_q$, see Fig. 8. Observe that the maximally crossed form of the diagram obeys the bosonization structure, that is, it satisfies (45). Every other bosonized diagram can be derived from it by a finite number of swaps of two c^\sharp -vertices, each amounting to 4 swaps of fermionic connectors. So the total number of fermionic swaps is divisible by 4 and thus even, which immediately yields $\text{sgn}(\xi, \pi_p, \pi_h) = 1$.

Finally, it remains to count the admissible diagrams, indexed by (ξ, π_p, π_h) , contributing to the r.h.s. . For this, observe that the topological structure of all contributing diagrams is the same in the following sense: We can transform any diagram into any other by changing the order in which S_{\pm} -vertices enter the diagram and swapping the two c^\sharp -vertices inside certain S_{\pm} -vertices. In total, there are 2^n ways to select in which of the n vertices S_{\pm} the two c^\sharp -vertices shall be swapped. Next, consider the order in which the S_{\pm} -vertices enter the diagram. At each contraction step $j \in \{1, \dots, n-1\}$, there are two S_{\pm} -vertices which may join the existing diagram at that point, out of which one can be

chosen. This renders 2^{n-1} distinct orders for the S_{\pm} -vertices. Thus, $\sum_{\xi} \sum_{(\pi_p, \pi_h)}$ yields 2^{2n-1} diagrams of identical value contributing to the r.h.s. of (47). So comparing with (23),

$$\begin{aligned} \text{r.h.s.} &= \sum_{\substack{n=2 \\ n:\text{even}}}^{\infty} \frac{2^{n-1}}{n!} \sum_{k \in \tilde{\mathcal{C}}^q \cap \mathbb{Z}^3} \frac{1}{n_{\alpha_q, k}^2} (K(k)^n)_{\alpha_q, \alpha_q} \\ &= \frac{1}{2} \sum_{k \in \tilde{\mathcal{C}}^q \cap \mathbb{Z}^3} \frac{1}{n_{\alpha_q, k}^2} (\cosh(2K(k)) - 1)_{\alpha_q, \alpha_q} = n_q^{(b)}, \end{aligned} \tag{67}$$

which establishes (47). □

Acknowledgments. This research was supported by the European Research Council (ERC) through the Starting Grant FERMIMATH, Grant Agreement No. 101040991 of Niels Benedikter. The author thanks Niels Benedikter for helpful discussions.

References

- [1] Benedikter, N. & Lill, S.: Momentum Distribution of a Fermi Gas in the Random Phase Approximation. *Preprint*, <https://arxiv.org/abs/2310.02706> (2023)
- [2] Benedikter, N., Nam, P.T., Porta, M., Schlein, B. & Seiringer, R.: Optimal Upper Bound for the Correlation Energy of a Fermi Gas in the Mean-Field Regime. *Commun. Math. Phys.* **374**, 2097–2150 (2020)
- [3] Benedikter, N., Nam, P.T., Porta, M., Schlein, B. & Seiringer, R.: Correlation Energy of a Weakly Interacting Fermi Gas. *Invent. Math.* **225**, 885–979 (2021)
- [4] Benedikter, N., Nam, P.T., Porta, M., Schlein, B. & Seiringer, R.: Bosonization of Fermionic Many-Body Dynamics. *Ann. Henri Poincaré* **23**, 1725—1764 (2022)
- [5] Benedikter, N., Porta, M., Schlein, B. & Seiringer, R.: Correlation Energy of a Weakly Interacting Fermi Gas with Large Interaction Potential. *Arch. Ration. Mech. Anal.* **247**, 65 (2023)
- [6] Bohm, D., Huang, K. & Pines, D.: Role of Subsidiary Conditions in the Collective Description of Electron Interactions. *Phys. Rev.* **107**, 71–80 (1957)
- [7] Bohm, D. & Pines, D.: A Collective Description of Electron Interactions: III. Coulomb Interactions in a Degenerate Electron Gas. *Phys. Rev.* **92**(3), 609–625 (1953)
- [8] Brooks, M. & Lill, S.: Friedrichs diagrams: bosonic and fermionic. *Lett. Math. Phys.* **113**, 101 (2023)

- [9] Christiansen, M.R., Hainzl, C. & Nam, P.T.: The Random Phase Approximation for Interacting Fermi Gases in the Mean-Field Regime. *Preprint*, <https://arxiv.org/abs/2106.11161> (2021)
- [10] Christiansen, M.R., Hainzl, C. & Nam, P.T.: On the effective quasi-bosonic Hamiltonian of the electron gas: collective excitations and plasmon modes. *Lett. Math. Phys.* **112**, 114 (2022)
- [11] Christiansen, M.R., Hainzl, C. & Nam, P.T.: The Gell-Mann–Brueckner Formula for the Correlation Energy of the Electron Gas: A Rigorous Upper Bound in the Mean-Field Regime. *Commun. Math. Phys.* **401**, 1469–1529 (2023)
- [12] Coldwell-Horsfall, R.A. & Maradudin, A.A.: Zero-Point Energy of an Electron Lattice. *J. Math. Phys.* **1**(5), 395–404 (1960)
- [13] Coldwell-Horsfall, R.A. & Maradudin, A.A.: Erratum: Zero-Point Energy of an Electron Lattice. *J. Math. Phys.* **4**(4), 582 (1963)
- [14] Daniel, E. & Vosko, S.: Momentum Distribution of an Interacting Electron Gas. *Phys. Rev.* **120**(6), 2041–2044 (1960)
- [15] Dereziński, J. & Gérard, C.: Mathematics of Quantization and Quantum Fields. Cambridge University Press (2013)
- [16] Falconi, M., Giacomelli E.L., Hainzl, C. & Porta, M.: The Dilute Fermi Gas via Bogoliubov Theory. *Ann. Henri Poincaré* **22**, 2283–2353 (2021)
- [17] Feldman, J.S. & Osterwalder, K.: The Wightman Axioms and the Mass Gap for Weakly Coupled $(\phi^4)_3$ Quantum Field Theories. *Ann. Phys.* **97**, 80–135 (1976)
- [18] Friedrichs, K.O.: Perturbation of Spectra in Hilbert Space. *American Mathematical Soc.* (1965)
- [19] Gell-Mann, M. & Brueckner, K.A.: Correlation Energy of an Electron Gas at High Density. *Phys. Rev.* **106**(2), 364–368 (1957)
- [20] Giacomelli, E.L.: Bogoliubov theory for the dilute Fermi gas in three dimensions. In: M. Correggi, M. Falconi (eds.), *Quantum Mathematics II*, Springer INdAM Series 58. Springer, Singapore. (2022)
- [21] Giacomelli, E.L.: An optimal upper bound for the dilute Fermi gas in three dimensions. *J. Funct. Anal.* **285**(8), 110073 (2023)
- [22] Glimm, J.: Boson Fields with the ϕ^4 : Interaction in Three Dimensions. *Commun. Math. Phys.* **10**, 1–47 (1968)

- [23] Glimm, J. & Jaffe, A.: Positivity of the φ_3^4 Hamiltonian. *Fortschr. Phys.* **21**, 327–376 (1973)
- [24] Hepp, K.: Théorie de la renormalisation, Lecture Notes in Physics. Berlin Springer Verlag (1969)
- [25] Lam, J.: Correlation Energy of the Electron Gas at Metallic Densities. *Phys. Rev. B* **3**(6), 1910–1918 (1971)
- [26] Lam, J.: Momentum Distribution and Pair Correlation of the Electron Gas at Metallic Densities. *Phys. Rev. B* **3**(10), 3243–3248 (1971)
- [27] Lieb, E.H. & Mattis, D.C.: Exact Solution of a Many-Fermion System and Its Associated Boson Field. *J. Math. Phys.* **6**(2), 304–312 (1965)
- [28] Luttinger, J.M.: An Exactly Soluble Model of a Many-Fermion System. *J. Math. Phys.* **4**(9), 1154–1162 (1963)
- [29] Sawada, K.: Correlation Energy of an Electron Gas at High Density. *Phys. Rev.* **106**(2), 372–383 (1957)
- [30] Sawada, K., Brueckner, K.A., Fukuda, N. & Brout, R.: Correlation Energy of an Electron Gas at High Density: Plasma Oscillations. *Phys. Rev.* **108**(3), 507–514 (1957)